Segregation of xenon to dislocations and grain boundaries in uranium dioxide

P. V. Nerikar, D. C. Parfitt, L. A. Casillas Trujillo, D. A. Andersson, C. Unal, S. B. Sinnott, R. W. Grimes, B. P. Uberuaga, and C. R. Stanek

Phys. Rev. B **84**, 174105 — Published 9 November 2011

DOI: 10.1103/PhysRevB.84.174105

Segregation of xenon to dislocations and grain boundaries in uranium dioxide

P.V. Nerikar,[1] D. C. Parfitt,[2] L. A. Casillas Trujillo,[1] D. A. Andersson,[1] C. Unal,[1] S. B. Sinnott,[3] R. W. Grimes,[2] B. P. Uberuaga[1] and C. R. Stanek[1]

[1]Los Alamos National Laboratory, Los Alamos, New Mexico 87545, USA
[2]Department of Materials, Imperial College London, London SW7 2AZ, UK
[3]Department of Materials Science and Engineering, University of Florida, Gainesville, Florida 32611, USA

It is well known that Xe, being insoluble in UO_2, segregates to dislocations and grain boundaries, where bubbles may form resulting in fuel swelling. Less well known is how sensitive this segregation is to the structure of the dislocation or grain boundary. In this work, we employ pair potential calculations to examine Xe segregation to dislocations (edge and screw) and several representative grain boundaries (Σ5 tilt, Σ5 twist and random). Our calculations predict that the segregation trend depends significantly on the type of dislocation or grain boundary. In particular, we find that Xe prefers to segregate strongly to the random boundary as compared to the other two boundaries and to the screw dislocation rather than the edge. Furthermore, we observe that neither the volumetric strain nor the electrostatic potential of a site can be used to predict its segregation characteristics. These differences in segregation characteristics are expected to have important consequences for the retention and release of Xe in nuclear fuels. Finally, our results offer general insights into how atomic structure of extended defects influence species segregation.

I. INTRODUCTION

Segregation can be understood as the interaction between an isolated zero dimensional defect (in this case, an impurity) and multidimensional defects such as dislocations (1D), grain boundaries (GB) and free surfaces (3D).[11] The driving force for this process is the energy difference (segregation energy) between the isolated impurity in the bulk and that associated with an extended structural defect. If the energy at the structural defect site is lower than in the bulk, the local impurity concentration is higher at the structural defect than in bulk and conversely, if the energy at the defect site is higher than in the bulk, the impurity will remain in the bulk. Segregation phenomena influence many material properties such as ion transport (which has a strong effect, for example on sintering rates), electrical and chemical reactivity and grain growth.[2] At higher concentrations, segregating impurities are known to form glassy or ordered phases and can cause structural transformations of the GB.[2, 3]

In the case of UO_2 nuclear fuel, fission gases such as xenon (Xe) are insoluble in the fuel matrix.[45] Therefore, Xe tends to segregate to dislocations and GBs forming fission gas bubbles. Xe may diffuse along the short circuit paths provided by these two defects and be released into the plenum region between the fuel rod and the cladding.[5] If the gases are released from the fuel, they contribute to the gaseous atmosphere within the fuel pin and the fuel pin internal pressure correspondingly increases; this can contribute to failure of the fuel pin. If these gases are retained inside the fuel, they form bubbles,

which lead to swelling of the fuel matrix. Swelling is detrimental to fuel performance as it contributes to fuel-cladding mechanical interaction (FCMI); the resulting stresses can shorten the lifetime of the pin.[7] Swelling and release are complementary phenomena and must be characterized together to gain a fundamental understanding of the complex effects of fission gas evolution.

Studies of segregation to dislocations are non-existent for ceramics, but are more common for metals. For example, the pinning of dislocations by implanted helium in aluminum[8] or niobium[9] shows the importance of segregation in determining both enhanced diffusion of atomic species and changes in mechanical properties of the bulk material. Metal-ceramic interfaces, which can be composed of ordered arrays of dislocations, have also been shown to act as energetically favorable nucleation points.[6, 7] Segregation to GBs in both metals and oxides has received significantly more attention. For a detailed review, see [1] and references within. More relevant to the work in this paper are segregation studies on fluorite-structured materials such as yttria-stabilized zirconia (YSZ). For example, Lei et al.[3] examined yttrium segregation to a 24° [001] GB in YSZ using a combination of Z-contrast scanning transmission electron microscopy (STEM) and electron energy loss spectroscopy (EELS). They observed an increase in the number of electrons in the GB plane due to formation of oxygen vacancies. Mao et al.[12] considered the segregation of yttrium (Y) to symmetric Σ5 tilt GBs in cubic zirconia (ZrO_2) using density functional theory (DFT). Y^{3+} segregation to Zr^{4+} sites in the GB was predicted to be energetically favorable compared to the bulk, in agreement with the experimental results of Dickey et al.[13]

It is clear, therefore, that segregation of external species to GBs and dislocations may play an important role in influencing material properties. This is especially true for UO_2 where segregation may affect fission gas distribution throughout a nuclear fuel grain. Despite this, segregation studies in UO_2 are lacking. Sonoda et al.[14] irradiated four UO_2 fuel discs at different burn-ups in order to identify the conditions for the formation of the rim structure. The microstructural evolution was observed through high resolution scanning electron microscopy and transmission electron microscopy. They observed the dislocations and GBs to be heavily decorated with fission gas bubbles. More recently, Chartier et al.[8] considered the incorporation of Xe as interstitial defects in different planes, Σ5 tilt GB, faceted and spherical voids, using empirical potentials. They predicted the GB and spherical shaped voids to be the most favorable for Xe incorporation. However, a detailed understanding of the dependence of segregation of fission products on the atomic details of the micro-structural defects in UO_2 is lacking. This provides the motivation for our work.

In a recent study, we provided atomistic results for relaxed structures of the Σ5 (310) tilt, Σ5 (001) twist and a random disordered GBs.[169] Similarly, in a separate recent paper,[10] we examined the energy and strain surrounding four typical dislocations in UO_2 using atomic scale simulations. Here, we utilize those results to explore the effect of GB and dislocation structures on Xe segregation. The goals of this study are to understand how Xe segregates to GBs and dislocations in UO_2 and to determine how sensitive this segregation behavior is to the structure of the dislocation or GB. The results from these atomistic simulations will in the future be applied to develop a mesoscale model that take into account a wider range of relevant microstructures that are currently inaccessible through atomistic methods.

While these results are specific to the problem of fission gas segregation to boundaries and dislocations in nuclear fuel, the issue of species segregation is a generic phenomenon, with consequences, as mentioned, for mass transport, grain growth kinetics, and electronic properties.[2] As such, our results offer generic insight into how differences in the atomic structure of these extended defects changes the interaction with impurity species in the material.

II. COMPUTATIONAL METHODS

Our computational approach uses Born-like atomic scale simulations with empirical pair potentials to describe the interaction between atom pairs. The simulations require accurate energy minimization of a given trial atomic configuration. Two different codes are used in the calculations. For the dislocation simulations, we use LAMMPS (Large-scale Atomic/Molecular Massively Parallel Simulator)[118] and for the simulations of GBs, we use the Los Alamos code CLSMAN. The strain field due to the dislocations propagates much further into the bulk crystal[19] than those surrounding GBs and hence much larger system sizes are required for the dislocation simulations, which are not accessible using CLSMAN. The LAMMPS code is more efficient for the large-scale dislocation simulations. Such complications do not arise for GB simulations. It is important to note that the results obtained from these two different codes are the same for a series of test Xe segregation calculations.

We use the U-O potential derved by Basak et al.[12] for the Xe segregation calculations. The Xe interaction with the uranium and oxygen atoms has been fit to DFT+U energies by Geng et al.[13] using a Lennard-Jones potential for Xe-Xe and Xe-O and a Born-Mayer term for the Xe-U interaction. Geng et al. used this potential to examine Xe (111) planar clustering in UO_2. From previous work,[14] it is known that the equilibrium solution site for Xe in stoichiometric UO_2 is a bound Schottky defect (a neutral tri-vacancy consisting of a uranium vacancy and two nearest neighbor oxygen vacancies) in UO_2, although in hyper-stoichiometric UO_{2+x} the equilibrium solution site is the isolated uranium vacancy.[22] For our segregation calculations, the Xe energy is calculated by replacing each uranium atom one-by-one with a Xe atom (Xe_U'''' in Kroger-Vink notation). This approach allows for the determination of a segregation profile (segregation energy as a function of distance from the extended defect), as has been done previously for surfaces in fluorite materials by Stanek et al.[15, 16] The justification for only considering uranium sites in the present work is that we are primarily interested in capturing relative trends and observing the effect of microstructure on segregation. However, we did perform a limited number of calculations where corresponding oxygen atoms (resulting in a bound Schottky defect) are removed to achieve electroneutrality. Even though the resulting values are different quantitatively, the relative stability of sites did not change, supporting our simplified approach of considering uranium vacancies. We also perform limited calculations, where Xe is incorporated in interstitial sites to make a comparison of the most stable Xe solution site as a function of stoichiometry.

It should be noted that there are a number of potentials that have been developed for UO_2; Govers et al.[17] give an overview of the performance of a number of them. Our choice of the Basak potential is based on our previous experience that it agrees

reasonably well with DFT calculations of GB structure.[18] Furthermore, the potential due to Basak et al. provides a good replication of the elastic constants leading to a more accurate representation of the strain energy. However, all of the UO_2 potentials are limited in their applicability and none of them are perfect. We expect that the qualitative trends we describe here are independent of the potential, though the details may differ. In our previous work on dislocations[10] we used the potential by Morelon et al.[19] (which reproduces the elastic constants less well). We note that the dislocation core structure, especially of the U ions, predicted by both the Morelon and the Basak potentials are very similar. Here, we also use the Basak potential for all calculations for convenience in comparing results for dislocations with grain boundaries.

1. Dislocation Calculations

The line energy of a dislocation varies with the square of the Burgers vector. Therefore we consider dislocations only along the close packed directions in UO_2. We further limit our calculations to a pure screw or edge dislocation. The line direction (or sense) of the screw dislocation occurs along the Burgers vector and therefore determines the geometry of the cell. For the pure edge dislocation, where the Burgers vector is perpendicular to the line direction, we assume that the line direction also occurred in a close packed direction. This produces an edge dislocation that slips along the {100} planes, which is found experimentally to be the dominant slip system in stoichiometric UO_2.[25] In all cases we orient the cubic UO_2 crystal such that the line of the dislocation lies along the *z*-axis (see figure captions for description of coordinate systems). For the screw dislocation this gives a Burgers vector of <110>. In the case of the edge dislocation we take the Burgers vector to be in the <110> direction and to lie along the y-axis (and slip, were it to occur, would take place on the (001) plane).

The cells containing the dislocations consist of a central cylindrical core region where atomic relaxations are calculated explicitly, a surrounding region where the ions are held fixed in the positions expected from elastic theory, and a vacuum gap that separates adjacent periodic cells. We terminate both the edge and screw dislocation cells with {100} and {110} planes: the {100} had half of the terminating oxygen ions removed in order to ensure a non-polar surface.[20] Both sets of simulation cells are initially constructed from a 35 × 55 × 9 supercell of the rotated unit cell, which gives a system size of around 20 × 22 × 3.5 nm, with a vacuum gap in the x and y directions and contiguous lattice in the z-direction. The displacement field found from the solution of the elastic strain field around the edge and screw dislocation is then applied to each of the cells.[2721] The ions that have distances greater than 8 nm from the centre of the cell are held fixed in these positions (i.e. 8 nm is the diameter of the core cylinder).

To calculate the segregation energy, a xenon atom is substituted onto each uranium ion site to produce several thousand individual calculations For each of these calculations the atoms not in the fixed region are displaced by 20 pm in a random direction and then minimized using a Polak-Ribiere variant conjugate gradient algorithm,[2822] as implemented in the LAMMPS code, until the variation in energy is less than 0.001 eV. In previous simulations of dislocations and GBs in UO_2,[10] it has been noted that the oxygen sub-lattice can display many closely spaced local minima. In establishing the segregation energy, these local minima will be evident as noise in the variation in segregation energy

from site to site; the calculated data show little scatter and therefore we are confident that the existence of these local minima did not significantly impact our conclusions.

2. Grain Boundary Calculations

We consider Xe segregation to the minimum energy structures of the Σ5 (310) tilt, Σ5 (001) twist and a random (110)(100) highly disordered GB, as determined in a previous study.[169] In that work, the minimum energy structures of the Σ5 (310) tilt and Σ5 (001) twist were found by calculating the γ-surface. In all cases, the GBs are oriented along the y-direction and the Xe profile is calculated along the z-direction. The structures thus found are employed for Xe segregation. The process of calculating the segregation energy for the GBs is similar to that for dislocations. We individually replace each of the uranium sites with Xe and calculate the total energy using a steepest descent minimization, as implemented in CLSMAN. As noted, we define the segregation energy as the difference in energy between any impurity in the bulk and at an extended structural defect. Our treatment of segregation is more rigorous than typical segregation studies by considering not just the different between bulk and GB, but also the explicit trend between bulk and GB. For example, as noted by Nowotny[29], hundreds of crystal layers near the GB or surface may be enriched by segregation in metal oxides and hence segregation related parameters should be resolved as a function of distance from the GB. Moreover, as predicted by Stanek et al.[23], although certain fission products do not segregate to surfaces in UO_2, they can get trapped just below the surface. Our methodological improvement is capable of accounting for such phenomena. (Nevertheless, our approach still only considers part of the complete segregation picture, as kinetic barriers to migration of fission products to dislocations and GBs are not taken into account.)

III. RESULTS

1. Segregation to Dislocations

The energy relative to the lowest energy site is calculated for the edge and screw dislocations and the results are shown in Figure 1 (a) and (c), respectively. Figures 1 (b) and (d) show a portion of a (100) plane cutting through the dislocation (at the centre of these cells) where the sites are colored by their relative energies with respect to the lowest energy site for each dislocation. For the screw dislocation, some of the Xe sites near the core did not converge with a conjugate gradient minimization and hence are not reported. All the atoms in this portion of the cell are allowed to relax fully; that is, they are not held fixed at their elastic response positions. Thus, the segregation energy is the difference between the energy of the Xe atom in the bulk and its value at the lowest energy site (at the core of the dislocation) and in the same supercell.[1] Consequently, the

[1] This procedure is similar to taking the difference in total energy of Xe at a dislocation site and at an isolated site in a perfect UO_2 lattice, but more directly accounts for cancellation of, for example, dipole errors.

segregation energy is the driving force to move a Xe_U defect from the bulk to the most stable site at the dislocation.

For both the dislocation types, the relative energy approaches a saturation value as the defect moves away from the dislocation core (Figure 1 (a) and (c)), indicating that away from the dislocation the defect behavior becomes bulk-like, as expected. It is not possible however to rule out a residual electrostatic interaction between the dislocation core and the Xe_U defect. The segregation energies in both figure 1 (a) and (c) do not fully saturate (never reach a bulk value) with the size of cell considered. This may be an effect of the size of cell considered (large as it is) or it may imply the existence of electrostatic effects, qualitatively similar to the effect observed for GBs, as discussed below. In either case, it is clear that this effect is small, and will not affect the overall segregation trend. Therefore, we choose a characteristic bulk-like site 50 Å away from the dislocation core. This is the interaction range for the dislocations, defined as the distance up to which the dislocation can influence bulk phenomena. This results in a segregation energy of ~2.7 eV and ~5.5 eV for the edge and screw dislocation respectively. The interaction range has an impact on preliminary mesocale simulations that will be discussed in a future paper.

For the edge dislocation, the relative energy falls to its lowest value close to the core and in the tensile region of the dislocation strain field. This is reasonably intuitive as Xe_U defects have a large, positive defect volume (i.e. a crystal expands upon incorporation of these defects) and do not form chemical bonds. In the compressive region, we may expect the defect energy to rise as large defects are unlikely to migrate to regions that are already hydrostatically compressed. However, this rise is mitigated by the ability of the lattice to relax into the dislocation core itself and therefore we do not see a strong correlation between the elastic strain field and the defect energy.

The screw dislocation does not possess significant regions of hydrostatic strain (in the purely elastic case it possesses none). As a result the extent of the perturbation is much less than in the case for the edge dislocation. In contrast, the segregation energy is substantially greater for the screw dislocation than for the edge dislocation (~5.5 compared with ~2.7 eV). This indicates that there are some sites at the core of the screw dislocation that are energetically very stable.

For both types of dislocations, there are several examples of sites with very different segregation energies that are spatially close to each other, particularly in the core region. We suggest that these differences are caused by different arrangements of oxygen ions around the segregation site. The influence of these differing oxygen arrangements will be discussed in more detail in Section IV.

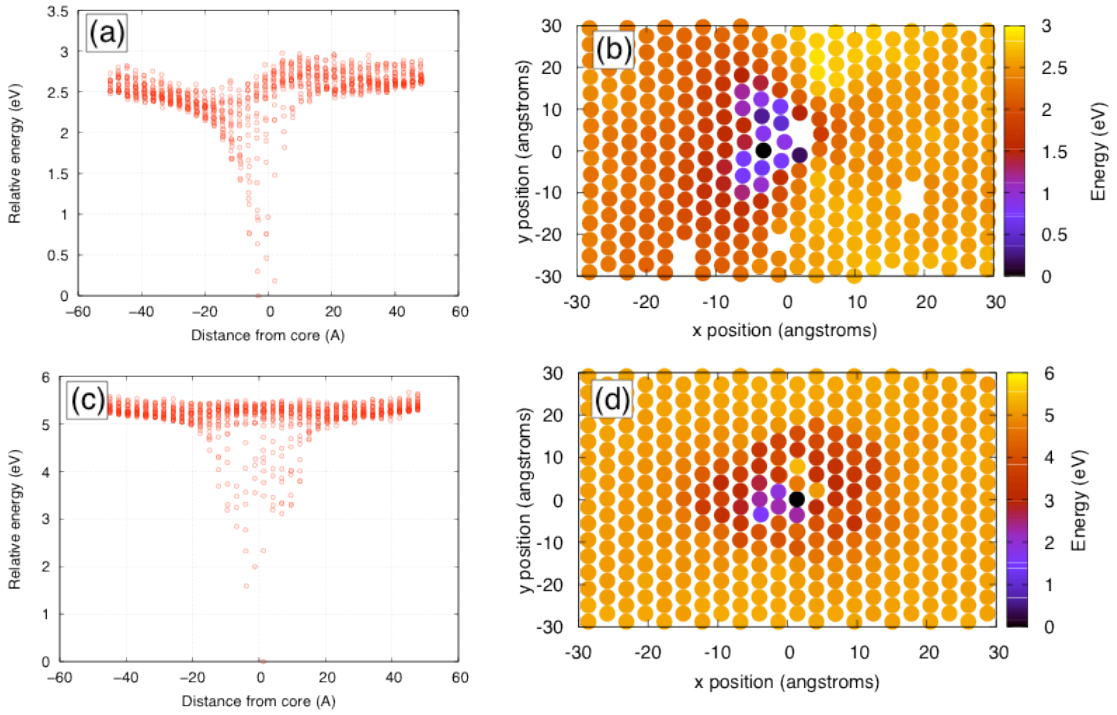

Fig. 1. Relative Xe energy versus distance for (a) an edge and (c) a screw dislocation in UO_2. (b) and (d) Color coded maps of (a) and (c) for the edge and screw dislocations respectively around the dislocation core where the sites are colored by their relative energies indicating the lowest energy (black) to the highest energy (yellow) sites. Each point is the position of a single Xe atom at a given site in the UO_2 host. In both cases, the dislocation line is along the z-axis of the coordinate system (out of the page).

2. Segregation to GBs

The relative energy versus distance is plotted for the Σ5 twist GB in Figure 2 (a) where the energy is presented relative to the lowest energy site. As we use periodic boundary conditions in our calculations, there are two GBs in the simulation cell at 0/90 Å and 45 Å. Figure 2 (b) illustrates a portion of Figure 2 (a) that is achieved by cutting through the GB (at the centre of the cell) where the coloring scheme is the same as that for dislocations. The color of each circle represents the energy of the Xe atom with respect to the lowest energy site. We predict that the lowest energy site is at the GB, which suggests that Xe has a tendency to segregate to the Σ5 twist GB in UO_2. The reason for this tendency is the decrease in the strain energy, which comes from the more open structure at the GB compared to the bulk. Recall that a Xe atom is large and insoluble in the bulk. Therefore, it prefers to reside at the GB, where the strain due to Xe is accommodated more readily than the bulk. This is also consistent with experimental observations and previous calculation results.[14] However, there are other aspects to note for Xe segregation to the twist GB. First, we predict that there are sites at the GB that are energetically unfavorable compared to the bulk. The range of energy of these sites at the

GB is between 0 to ~3 eV. This indicates that the sites at the GB are inequivalent in terms of the ease with which they can accommodate a Xe atom. It is interesting to note that both the lowest and the highest energy sites are at the GB. Second, the relative energy reaches a bulk value at ~20 Å from the GB. Moreover, the segregation energy for this GB is low (~1 eV). All these aspects will be discussed in more detail in Section IV.

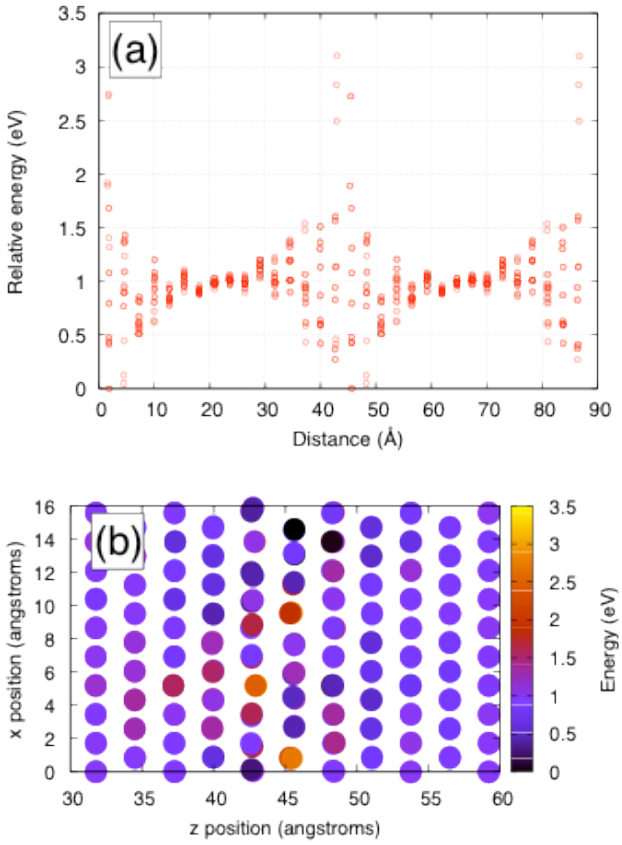

Fig. 2. (a) Relative Xe energy versus distance for the Σ5 twist GB in UO_2 and (b) a color coded map of (a) around the GB where the color scheme is the same as Fig 1. The GBs are at 0/90 Å and 45 Å. The grain boundary normal lies along the z direction and the grain boundary plane lies in the x-y plane.

The calculated segregation profile for the random GB is plotted next in Figure 3 (a) and (b). The positions for the two GBs are ~25 Å and 60 Å for this supercell. The general trend is similar to that for the twist GB in that there is a range of Xe energies at the GB. That there are multiple inequivalent sites for Xe at the boundaries is consistent with the general picture of a GB being composed of different structural units.[30] Depending on the position of any site in the GB, the atomic interaction (uranium and oxygen in this case) will change and this will strongly affect the segregation characteristics. These differences in oxygen environment for every uranium site results in a large range of energies (~8 eV) at the GB. It can be observed that even in the bulk, for each particular distance from the GB there is a range of energies for Xe segregation (~ 1.5 eV), which increases as the GB is approached as illustrated in Figure 3 (b). This indicates that the presence of GBs is

influencing bulk phenomena and the size of the cell considered may not be large enough. The scatter in the calculated data, however, is substantially smaller than the segregation energy. The segregation energy is ~6.5 eV indicating that Xe will strongly segregate to the GB. The interaction range for the random GB is ~15 Å.

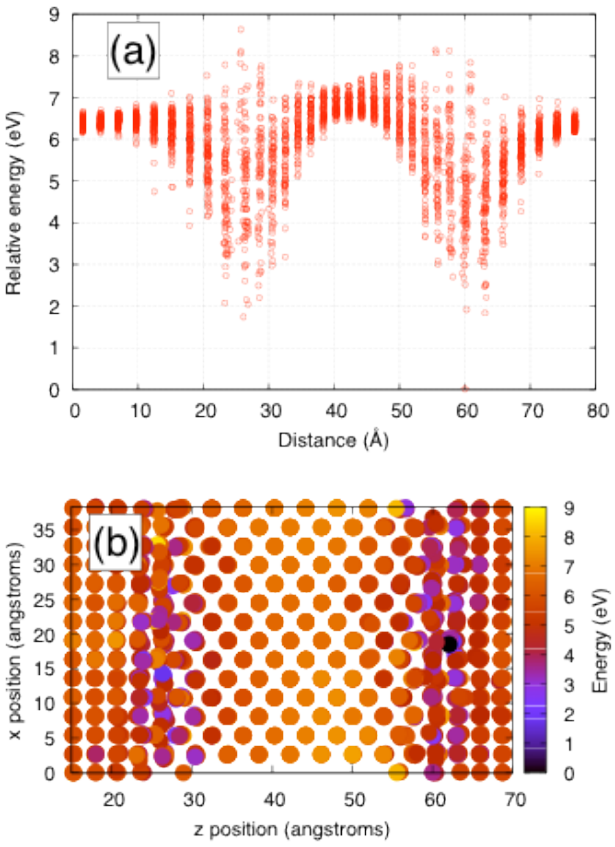

Fig. 3. (a) Relative energy of Xe in UO_2 as a function of distance for the random GB, and (b) a color coded map of (a) around the GB where the color scheme is the same as Fig 1. The GBs are at ~25 Å and 60 Å. The grain boundary normal lies along the z direction and the grain boundary plane lies in the x-y plane.

In previous studies,[16,31] we observed that the lowest energy structure found on the γ-surface for the Σ5 tilt GB exhibits a slight asymmetry arising from a reconstruction of the symmetric structure of the GB. This reconstruction gives rise to an electrostatic potential drop across the grain that results in several aspects of Xe segregation that are not present in Σ5 twist and random GBs. For example, as can be observed from Figure 4 (a), the Xe segregation profile for the Σ5 tilt GB does not exhibit bulk-like behavior in contrast to the profiles of Σ5 twist and random GBs. In other words, the relative energy does not plateau far away from the GB. We verify this by calculating the segregation profile in larger grain sizes (~40 nm) (Fig. 5) and also in cells where the in-plane dimensions were doubled compared to the present calculation (not shown). This trend is similar to the result obtained in our previous work[31] where we observed that the electrostatic potential

is independent of the grain size. As indicated in Figure 4 (b), all the sites at the GB are energetically favorable compared to the bulk and Xe will always segregate to the GB. The scatter of energy in the bulk is low, suggesting that all the uranium sites in the bulk are accommodating strain in a similar manner. The segregation energy for a characteristic bulk-like site is ~4 eV and the interaction range is ~55 Å for the particular grain size considered. Obviously, the interaction range for the particular GB is system size dependent since the electrostatic potential is long range.

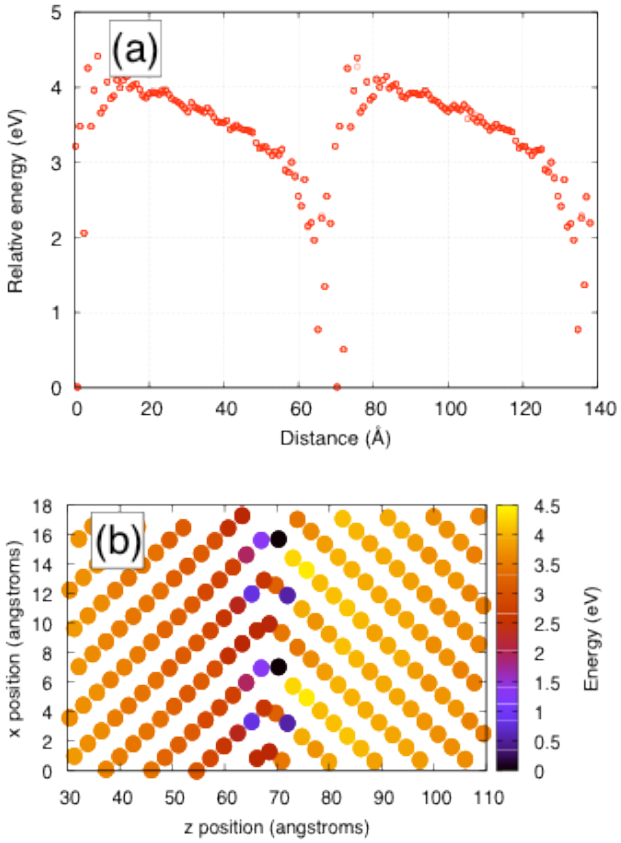

Fig. 4. (a) Relative energy versus distance for the Σ5 tilt GB, and (b) a color coded map of (a) around the GB where the color scheme is the same as Fig 1. The grain boundary normal lies along the z direction and the grain boundary plane lies in the x-y plane.

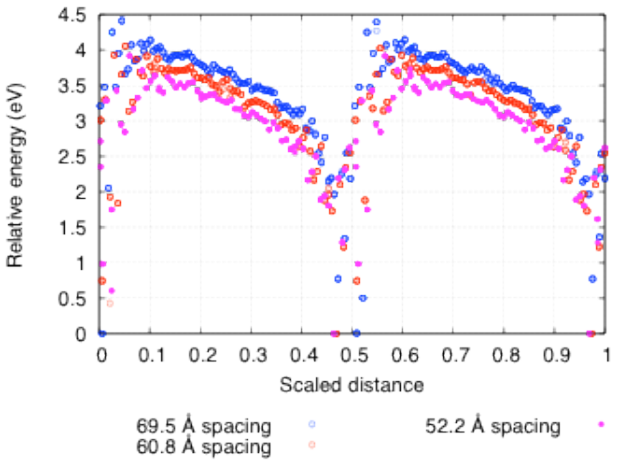

Fig. 5. Xe segregation energy profile near the Σ5 tilt GB as a function of system size. As can be seen, the trends are independent of the system size. The offsets between the three curves are a consequence of the electrostatic potential generated in the grain interiors by the asymmetric nature of the grain boundary. Limited calculations on systems with spacings as large as 200 Å reveal the same physical trends.

Thus, in spite of calculations on larger grain sizes, the relative energy does not reach a bulk-like value and, additionally, the segregation trend is asymmetric. To further understand this issue, we calculate the relative energy of a uranium vacancy as shown in Fig. 6(a). The segregation profile has the same form as that of Xe segregation. This is expected since both defects (Xe and uranium vacancy) have a charge of -2.4 (within the Basak potential) relative to the perfect UO_2 lattice and are similarly affected by the electrostatic potential drop across the grain. However, the calculated incorporation energy[23] (Figure 6(b)), which is the difference between the two curves, does not exhibit any asymmetry. Additionally, we obtain an incorporation energy of ~ 5.73 eV in the grain. This value is similar to the calculated incorporation energy of Xe in bulk UO_2, shown by a straight line in the plot. This result implies that electrostatic effects are present for this GB and play an important role in determining segregation behavior. A surprising point to note is that the incorporation energy for a significant fraction of sites increases at the GB. This in turn means that for these sites, Xe prefers to be in the bulk rather than at the GB. That is, if vacancies already exist, Xe prefers to fill the vacancy in the grain interior rather than the one at the boundary. However, once it has filled it, the Xe-vacancy complex further lowers its energy by moving to the boundary. It is worth pointing out that intrinsic defects such as Schottky trios and extrinsic impurities such as Zr^{4+}, which are charge neutral with respect to a perfect UO_2 lattice, will not be affected to a significant extent by the electrostatic potential drop. Pure strain effects will dominate the segregation of these defects according to the traditional McLean isotherm model.[32]

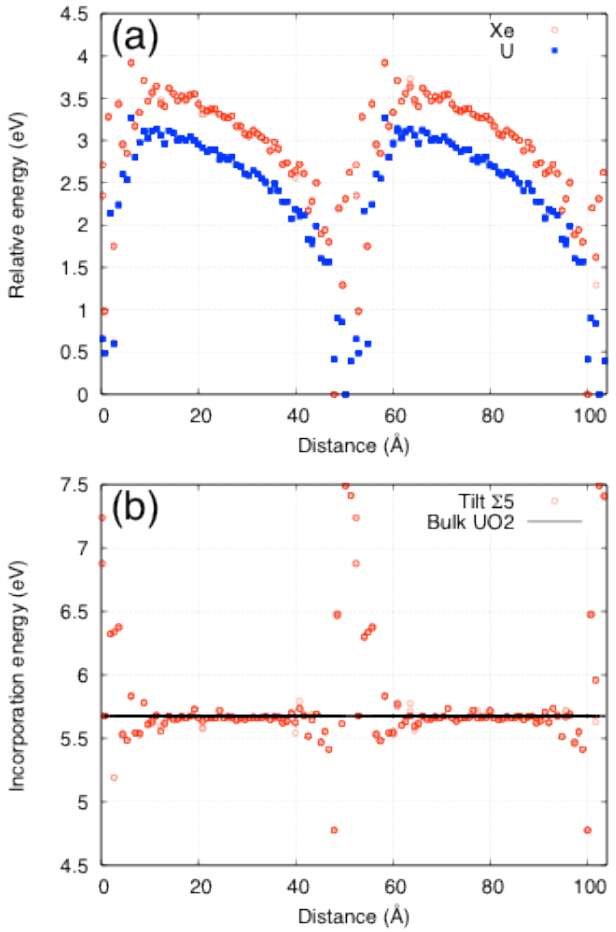

Fig. 6. (a) Relative uranium vacancy energy and relative Xe energy versus distance for the Σ5 tilt GB, with the Xe segregation profile shown for comparison and (b) incorporation energy of Xe versus distance. The bulk incorporation energy is indicated by the solid line.

As discussed above, the results indicate that the electrostatic effects are important for the Σ5 tilt GB. There are two major contributions to the segregation energy in ceramics.[1] The first is the elastic contribution, which occurs due to relaxation of atoms around a segregating impurity to relieve induced elastic strain. The second component of the segregation energy is due to the ionic nature of species in many ceramics and is an electrostatic contribution. Typically in ceramics, the formation energies of cation and anion vacancies at the GB are different and generally lower compared to the bulk. This results in an electrostatic potential due to preferential charged defect segregation to the GB (so called space charge). The impurity segregation energies then depend on this long range potential. In our case, the effect of the electrostatic potential at the GB on segregation of Xe is similar to that of the traditional space charge. However, the cause of the electrostatic potential is the atomic structure of the GB itself and not the segregation of defects to the GB. To quantify the effect of each contribution, we divide the segregation energy into individual components in Figure 7. The electrostatic potential associated with a given ion is the measure of the Coulomb interaction per unit charge experienced by that ion. For the empirical-potential calculations, this is directly related to

the total energy of the system, being a sum of the products of the charge of each ion (2.4 for uranium within the Basak potential) and the electrostatic potential at the position of that ion. The elastic contribution for any particular ion is the difference between the total energy and the electrostatic contribution. In particular, the electrostatic contribution varies linearly across the grain while the elastic component has the typical symmetric segregation profile across each grain, i.e. the energy reaches a bulk value of ~2.8 eV at a distance of 25 Å from the GB. This figure clearly illustrates that it is the electrostatic contribution that causes the asymmetry and changes the interaction range for this particular GB. For the other two GBs, the electrostatic contribution is not large enough to influence segregation trends to any significant extent.

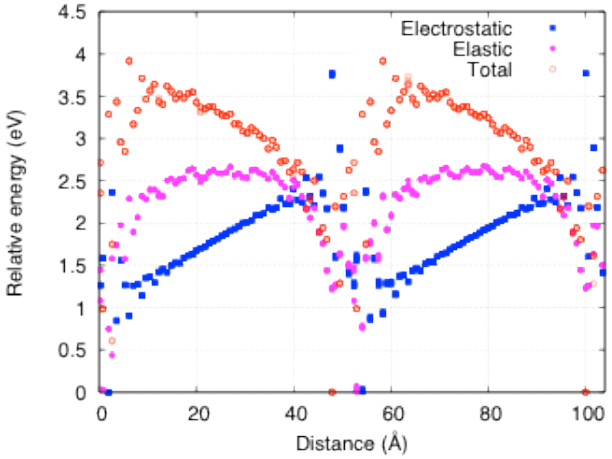

Fig. 7. Electrostatic and elastic components of the segregation energy of Xe to the Σ5 tilt GB.

IV. DISCUSSION

This work builds on our previous findings regarding the structures and energetics of dislocations (edge and screw)[17] and GBs (Σ5 tilt, Σ5 twist and random)[16] in UO_2. The objective here is to explore the sensitivity of the segregation behavior of Xe to details of the atomic structure of dislocations and GBs. For both dislocations and GBs, the lowest energy site is always at the extended defect, implying that Xe will always segregate to the defect. An interesting point to note is that the relative energy never reaches a bulk value implying the existence of electrostatic effects for both dislocations, similar to the Σ5 tilt GB, However, there are significant differences in the segregation characteristics of dislocations and GBs. For both the dislocations, all the sites at the dislocation core have a relative energy equal to or lower compared to the sites in the bulk. This is in contrast to the segregation profiles for the Σ5 twist and random GBs where some sites are unfavorable compared to the bulk. To compare the segregation characteristics of the extended defects (dislocations and GBs), we present the segregation energy, defined as the difference in energy of a Xe atom in the bulk and the most stable site of the structural defect, given in Table 1. The results predict that Xe strongly prefers to be in the random, highly disordered GB, followed by the screw dislocation. There also seems to be a rough correlation between the segregation energy and previously calculated GB formation

energy.[16] These results indicate that for a GB of low energy, the segregation energy would also be low. This makes physical sense since GBs with low interfacial energies have a smaller misfit and hence a lower propensity towards impurity segregation.[2] Hence, Xe does not prefer the GB strongly to the bulk in the Σ5 twist GB case. For the two Σ GBs, the orientation of the grains with respect to each other affects the GB energy and consequently the segregation energy. Similarly, it takes a higher energy to form the random GB and Xe segregates more strongly to this GB. Based on this result, segregation characteristics of other GBs in UO_2 may be predicted. Such a correlation may also exist in other materials. However, as fission products accumulate through burn-up and segregate to GBs, they will alter the energetics of the boundaries and through this may influence the fission gas evolution of the fuel.

TABLE I. Grain boundary and dislocation formation and segregation energies of the extended defects considered in this study.

Defect Site	**Formation Energy**[16-17]	**Segregation Energy (eV)**
Edge Dislocation	2.19 eV/Å	2.7
Screw Dislocation	1.87 eV/Å	5.5
Σ5 twist GB	0.073 eV/Å^2	0.97
Σ5 tilt GB	0.099 eV/Å^2	4.09
Random GB	0.116 eV/Å^2	6.42

As mentioned in the previous section, each uranium site at the core of a dislocation or the plane of a GB has a different oxygen environment, i.e., each site has a different oxygen arrangement around it that affects segregation properties. The distortions away from ideal atomic arrangements manifest as strain and thus, to determine if there is a correlation between the strain associated with a given segregation site and the segregation energy, we calculate the volumetric strain for each uranium site. For this, first we construct the ideal (unrelaxed) oxygen arrangement around each uranium site and then compare this arrangement to the oxygen atom positions in the relaxed structure, solving for the transformation matrix in a least-squares sense from which the volumetric strain can be calculated. For example, if the oxygen arrangement in the relaxed structure for a particular site matches that in ideal fluorite, then the volumetric strain will be zero. The other factor that influences segregation within these ionic oxides is the electrostatic potential. Therefore, in Fig. 8a, we plot the segregation energy of Xe near the Σ5 tilt GB as a function of electrostatic potential while the segregation energy of Xe vs strain is shown in Fig. 8c. In Fig. 8e, the segregation energy versus strain is plotted for the edge dislocation (the dislocation structure is too large to be optimized in GULP[33] to calculate the electrostatic potential). For the tilt GB, both strain (open symbols) and electrostatic potential (closed symbols) are divided into bulk and GB regions. Bulk (for both GB and dislocation) is defined as a region with a strain limit of 0.01, i.e. where the distortion of the oxygen arrangement is negligible (see Figs. 8b, 8d and 8f).

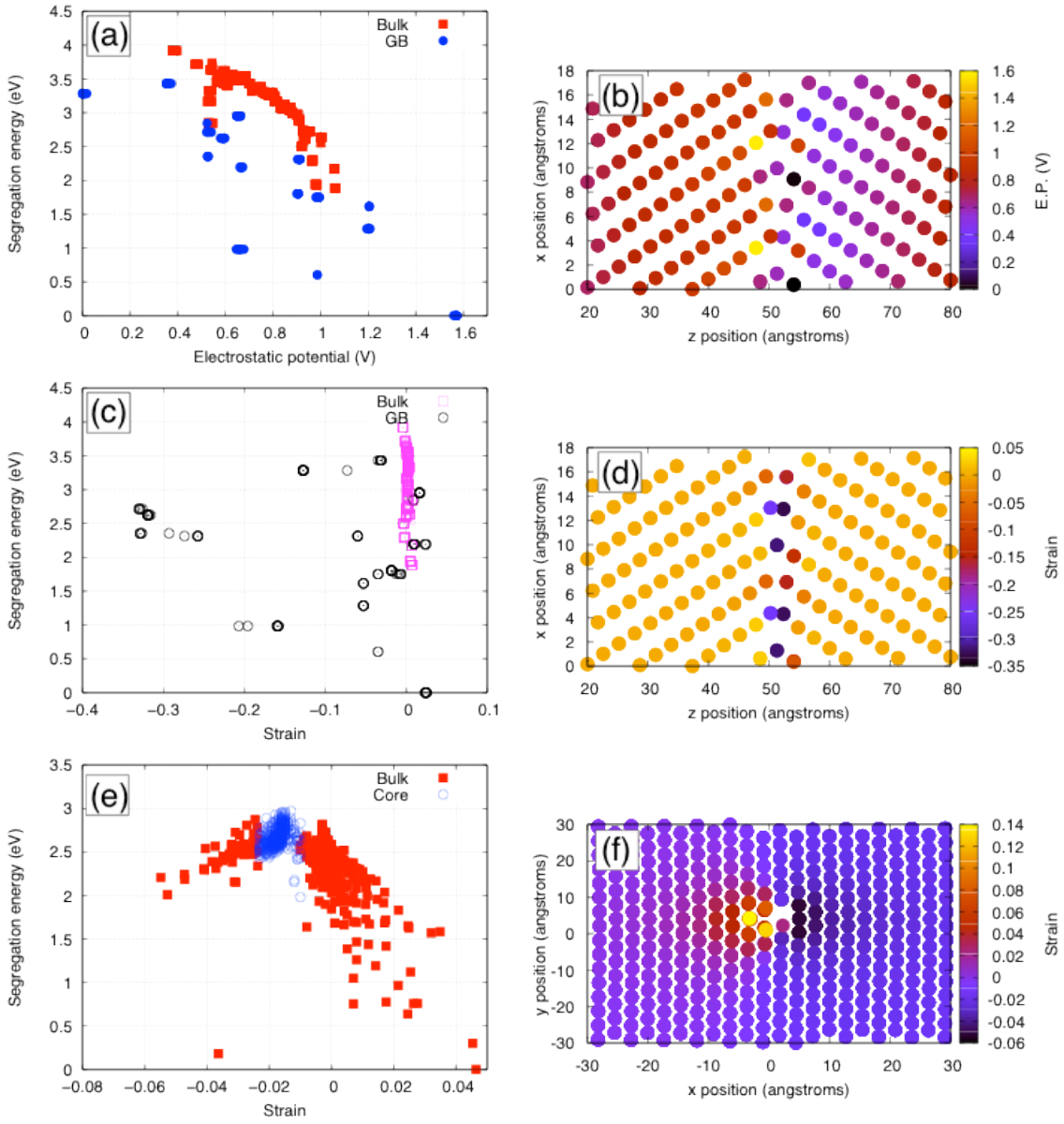

Fig. 8. Xe segregation energy versus (a) electrostatic potential (EP) and (c) strain for the Σ5 tilt GB with corresponding color-coded maps of (b) the electrostatic potential and (d) strain versus distance for the Σ5 tilt GB. (e) Xe segregation energy versus strain for the edge dislocation, and (f) color-coded map of strain versus distance for the edge dislocation.

First, if we examine how the Xe segregation energy correlates with electrostatic potential, we see that Xe segregation correlates independently in both the bulk and GB regions. That is, there are two trends, one in which the Xe segregation energy in the bulk region of the system correlates with the electrostatic potential and another where it correlates with the electrostatic potential in the GB region. The correlations with strain are much less pronounced. There is a rough correlation in that the lowest energy site is in a tensile region while sites with higher energies are under compressive strain. This

physically makes sense since large defects such as Xe are unlikely to segregate to regions that are already hydrostatically compressed. Clearly the behavior in the bulk is dominated by the electrostatic potential, as there is no correlation with strain. However, even near the GB, the correlation with electrostatic potential is still greater than with strain. Neither, though, can be used to predict the overall segregation trends.

For the edge dislocation, we observe a similar trend as for the tilt GB that in general sites under compressive strain have high segregation energies in both the bulk and GB regions. However, again, a clear trend that could be used to predict segregation energies is not established. Similar characteristics are also observed for the screw dislocation and the other two GBs.

This analysis for both dislocation and GB shows that any assumption about the segregation characteristics of any site just based on either the electrostatic potential or the strain on that site would be approximate at best and would lack connection to the behavior apparent at the atomic level. This work thus highlights the importance of atomistic calculations.

Chartier et al.[8] considered the incorporation of Xe to the minimum energy structure of the Σ5 tilt GB in UO_2 using the Morelon potential. Their minimum energy structure has intrinsic Schottky defects along the GB in which they incorporate Xe as interstitials. Their results predict that Xe prefers to be in the Σ5 tilt GB, similar to our predicted results. However, they incorporate multiple Xe atoms along the GB. Moreover, no defects were created for this incorporation as they considered interstitial positions. Thus, owing to the differences in the method of incorporation and empirical potential, a direct comparison between their and our results cannot be made.

However, motivated by this, we calculate the segregation profile for the Σ5 tilt GB similar to Figure 4 (a) where now we incorporate Xe in the interstitial sites. We then calculate the solution energy of Xe as a function of stoichiometry both in the bulk and at the GB according to the defect equilibria[23] as indicated in Table 2. This enables us to make a direct comparison of the most stable solution site (amongst either U vacancies or interstitials) for Xe as a function of stoichiometry. We calculate the formation energy of uranium vacancy in the bulk using the results of defect equilibria[22]. The formation energy of a uranium vacancy in the GB is taken as a difference of the bulk value and the segregation energy of uranium vacancy (Figure 5 (a)). This procedure is followed because it would be difficult to determine the most stable Schottky and oxygen Frenkel defect at the GB as required by the defect equilibria model.

The first thing to note in Table 2 is that the solution energy at the interstitial site is independent of stoichiometry, as no defects have to be created. Comparing the two bulk sites, Xe prefers to be in the uranium vacancy site for all stoichiometries. However, when considering Xe solution at the GB, the preferred site does depend on stoichiometry. In hypostoichimetric conditions, Xe prefers to be in the interstitial site at the GB compared to the uranium vacancy site. As we approach hyperstoichiometric conditions, it becomes energetically favorable to form uranium vacancies and hence the vacancy to become the most stable solution site. This may have implications for how Xe bubbles form at the GB as a function of stoichiometry. Moreover, the inclusion of bound Schottky defects as possible trap sites may change the current conclusions.

TABLE II. Solution energy of Xe as a function of stoichiometry for the interstitial and uranium vacancy sites for the cell with Σ5 tilt GB. For the bulk sites, the most stable solution site for each stoichiometry is shown in bold. For the GB sites, the value is shown in bold and has been italicized.

Defect Site	**UO_{2-x}**	**UO_2**	**UO_{2+x}**
Interstitial Bulk	20.05	20.05	20.05
Interstitial GB	***10.3***	10.3	10.3
Uranium vacancy Bulk	**16.48**	**10.48**	**4.48**
Uranium vacancy GB	12.46	***6.46***	***0.46***

The future goal of this work would be to use these atomistic results to provide an improved input to a thermodynamic mesoscale model, which will explore the competition between different sinks such as, for example, between dislocations and GBs. Our calculations predict that Xe segregates more strongly to the screw dislocation as compared to the edge dislocation. The random GB has an even higher segregation energy (6.42 eV). Therefore, based on our atomistic results, Xe will preferentially segregate to the random GB and then to the screw dislocation, in absence of kinetic factors. Moreover, the Σ5 tilt GB, owing to the existence of electrostatic effects, has a longer interaction range and may be able to reach further into the bulk to attract Xe. Further, each extended defect has at least one deep trap site. This has implications for the accumulation of Xe at the extended defect since the concentration of Xe will depend on the availability in the number of low energy sites as well as the characteristic energy of each site. Xe diffusion along the extended defect will also be influenced by the energetics of site preference. It is generally assumed that diffusion along the defect is easier compared to the bulk due to the open volume in the dislocation or GB. However, if Xe is trapped at such as a site, it would be energetically unfavorable to displace the Xe atom from that site and in turn would make Xe transport more difficult as compared to the bulk. Finally, segregation energies will probably change in the presence of multiple Xe atoms. All these aspects will be discussed as part of a future study.

Related to the question of Xe transport is the influence of finite temperature on our results. We have calculated 0K segregation energy profiles for Xe near a number of extended defect structures. The question naturally arises about the role of temperature in further modifying the behavior of Xe near these defects. As mentioned above, we expect the transport of Xe at and near these defects to be rather complicated, due to the existence of trap-like states. Further, the barriers for Xe migration might be modified by the strain fields associated with these defects, similar to what we observed for point defects in Cu.[24] However, the primary consequence of temperature is that Xe will not always be able to reach the most thermodynamically preferred state. For example, we predict that the random GB has the largest "sink" strength for Xe – the segregation energy for Xe is greatest to this boundary. However, kinetically, Xe will most likely become trapped at the closest sink, given a strong enough sink strength. Thus, if there is a greater number of twist GBs, there might be more Xe trapped at these boundaries than at the random boundaries, even though, thermodynamically, there is a greater tendency for Xe to be at

those boundaries. These effects, however, are not easily assessed with atomistic simulations and require higher level models, which is the subject of ongoing work.

Finally, it is useful to consider our work in a broader context. We have discussed how Xe segregation to dislocations and, in particular, grain boundaries depends very sensitively on the structure of those extended defects. In the case of the grain boundaries, we find that the Xe segregation energies vary by many eV depending on the structure of the boundary. As discussed, this will have implications for the microstructural evolution of the fuel; however, this sensitivity in the segregation of species to the boundary properties is a generic feature of all materials and all impurity/dopant species. Indeed, other work has found that the interaction of point defects with boundaries and interfaces depends on the properties of the boundary.[25, 26] In this sense, our results offer more general insight into this fundamental problem. For example, radiation induced segregation (RIS) is a primary concern with the performance of certain structural materials, such as ferritic[27] and austenitic stainless steels[28], and is the chief reason these materials are not used in reactors today. Our work shows that phenomenon such as RIS would be very sensitive to the microstructure of the material and that, in principle, RIS could be mitigated to some degree by engineering different types of microstructure into the material. Of course, more work is needed to more fully understand this, but the insights gained from this and related work offer one path forward for designing materials with enhanced radiation tolerance.

V. CONCLUSIONS

This work is part of a comprehensive study undertaken to explore the effect of microstructure on segregation characteristics of Xe in UO_2. Previously determined atomic structures of dislocations (edge and screw) and GBs (Σ5 tilt, Σ5 twist and random) are used to examine Xe segregation in which every uranium site is replaced by one by one with a Xe atom. It is predicted that Xe would preferentially segregate to all the structural defects (dislocations and GBs). Furthermore, for all the structural defects, there is one deep trap site at the core, which may have implications for Xe transport along the defect. However, this tendency for segregation depends on the detailed atomic structure of each defect. While Xe segregation to the screw dislocation is stronger as compared to the edge dislocation, it is observed that the segregation of Xe is strongest to the random GB among the GBs considered. A correlation between the GB energy and segregation energy is also observed, which could be exploited to predict segregation characteristics of other GBs. For both edge dislocation and Σ5 tilt GB, the lowest segregation energy site is observed to be in a region of tensile strain while higher energy sites are under compressive strain. Electrostatics plays a dominant role in determining the segregation characteristics of the Σ5 tilt GB. However, neither the strain nor the electrostatic potential can be used to predict the overall segregation trend. Further, the most stable solution site as a function of stoichiometry is calculated for the Σ5 tilt GB. It is predicted that Xe preferred to be in the uranium vacancy compared to the interstitial site in stoichiometric and hyperstoichimetric conditions, which may have consequences for how Xe bubbles form at the GB. The main impact of this work is that the segregation energies calculated using empirical potentials can be used directly in a higher length and time scale model to predict retention and release phenomena in nuclear fuels, as will be discussed as part of a future study.

ACKNOWLEDGEMENTS

Computational work at LANL was sponsored by the Nuclear Energy Advanced Modeling and Simulation (NEAMS) program. P.V.N. also gratefully acknowledges support from the Seaborg Institute at Los Alamos National Laboratory. P. V. N. would also like to thank Arthur Voter for providing access to the CLSMAN code. Los Alamos National Laboratory, an affirmative action/equal opportunity employer, is operated by Los Alamos National Security, LLC, for the National Nuclear Security Administration of the U.S. Department of Energy under contract DE-AC52-06NA25396. Computational work at Imperial College was partly funded by the European Commission through the FP7 F-BRIDGE project (Contract No. 211690). RWG is grateful to the EPSRC for funding under grant EP/I003320/1.

References

1 P. A. Dowben, *Surface Segregation phenomena* (CRC Press, 1990).

2 Y. Lei, Y. Ito, N. D. Browning, and T. J. Mazanec, Journal of the American Ceramic Society **85**, 2359 (2002).

3 Y. Yan, M. F. Chisholm, G. Duscher, A. Maiti, S. J. Pennycook, and S. T. Pantelides, Physical Review Letters **81**, 3675 (1998).

4 D. R. Olander, *Fundamental Aspects of Nuclear Reactor Fuel Elements*, Springfield, Virginia, 1985).

5 D. R. Olander and P. Van Uffelen, Journal of Nuclear Materials **288**, 137 (2001).

6 D. A. Shashkov, M. F. Chisholm, and D. N. Seidman, Acta Materialia **47**, 3939 (1999).

7 D. A. Shashkov, D. A. Muller, and D. N. Seidman, Acta Materialia **47**, 3953 (1999).

8 A. Chartier, L. Van Brutzel, and M. Freyss, Physical Review B **81**, 174111 (2010).

9 P. V. Nerikar, et al., Journal of the American Ceramic Society **94**, 1893 (2011).

10 D. C. Parfitt, C. L. Bishop, M. R. Wenman, and R. W. Grimes, Journal of Physics-Condensed Matter **22**, 175004 (2010).

11 S. Plimpton, Journal of Computational Physics **117**, 1 (1995) (http://lammps.sandia.gov).

12 C. B. Basak, A. K. Sengupta, and H. S. Kamath, Journal of Alloys and Compounds **360**, 210 (2003).

13 H. Y. Geng, Y. Chen, Y. Kaneta, and M. Kinoshita, Journal of Alloys and Compounds **457**, 465 (2008).

14 P. V. Nerikar, X. Y. Liu, B. P. Uberuaga, C. R. Stanek, S. R. Phillpot, and S. B. Sinnott, Journal of Physics-Condensed Matter **21**, 435602 (2009).

15 C. R. Stanek, M. R. Bradford, and R. W. Grimes, Journal of Physics-Condensed Matter **16**, S2699 (2004).

16 C. R. Stanek, R. W. Grimes, M. J. D. Rushton, K. J. McClellan, and R. D. Rawlings, Philosophical Magazine Letters **85**, 445 (2005).

[17] K. Govers, S. Lemehov, M. Hou, and M. Verwerft, Journal of Nuclear Materials **366**, 161 (2007).
[18] P. Nerikar, C. R. Stanek, S. R. Phillpot, S. B. Sinnott, and B. P. Uberuaga, Physical Review B **81**, 064111 (2010).
[19] N.-D. Morelon, D. Ghaleb, J.-M. Delaye, and L. V. Brutzel, Philosophical Magazine **83**, 1533 (2003).
[20] A. H. H. Tan, R. W. Grimes, and S. Owens, Journal of Nuclear Materials **344**, 13 (2005).
[21] J. P. Hirth and J. Lothe, *Theory of Dislocations* (John Wiley and Sons, 1982).
[22] E. Polak, *Computational Methods in Optimisation* (New York Academic Press, 1971).
[23] R. W. Grimes and C. R. A. Catlow, Philosophical Transactions of the Royal Society: Physical and Engineering Sciences **335**, 609 (1991).
[24] X. M. Bai, A. F. Voter, R. G. Hoagland, M. Nastasi, and B. P. Uberuaga, Science **327**, 1631 (2010).
[25] M. J. Demkowicz, R. G. Hoagland, and J. P. Hirth, Physical Review Letters **100**, 136102 (2008).
[26] A. Misra, M. J. Demkowicz, X. Zhang, and R. G. Hoagland, Journal of the Minerals, Meals and Materials Society **59**, 62 (2007).
[27] Z. Lu, R. G. Faulkner, and P. E. J. Flewitt, Materials Science and Engineering A **437**, 306 (2006).
[28] J. T. Busby, G. S. Was, and E. A. Kenik, Journal of Nuclear Materials **302**, 20 (2002).